Jet spectroscopy of anthracene and deuterated anthracenes

W. R. Lambert,[a] P. M. Felker,[b] J. A. Syage, and A. H. Zewail[c]
Arthur Amos Noyes Laboratory of Chemical Physics,[d] California Institute of Technology, Pasadena, California 91125

(Received 23 November 1983; accepted 8 December 1983)

Fluorescence excitation and SVL fluorescence spectra of jet-cooled h_{10}-, $9d_1$-, $9,10d_2$-, and d_{10}-anthracene are reported. Ground state vibrational assignments are presented for all these species and are compared with literature values. In addition, assignments for the first excited singlet state of h_{10}-anthracene are made using SVL spectra and rotational band contours as guides. The work presented herein serves as an essential reference for other work from this research group concerning the dynamics of excited anthracene (see accompanying papers), and completes the spectroscopy of the polyacene series.

I. INTRODUCTION

The study of large, isolated molecules in supersonic jets has revealed many new and important features of the spectroscopy and dynamics of such species. In this laboratory, we have been concerned primarily with intramolecular photophysical and photochemical processes as studied by picosecond time-resolved spectroscopy.[1,2] Of particular interest has been the study of anthracene,[1,2(g)] in which we have observed quantum beat-modulated decays. In the course of this work, we have found it necessary to make a comprehensive study of the spectroscopy of this large molecule in order to better understand the excited state dynamics. Although high resolution absorption and emission spectra have previously been obtained for h_{10}- and d_{10}- anthracene in mixed crystals[3,4] and in Shpolskii matrices,[4,5] the spectral structure is complicated by phonon coupling and/or the presence of multiple lattice sites. Furthermore, vibrational frequencies and Franck–Condon factors are likely to be perturbed by matrix interactions. Bulb experiments on anthracene yield primarily diffuse spectra[6] due to the prevalence of vibrational hot bands and sequence transitions. In the jet, however, the problems associated with matrix interactions and bulb thermal congestion are eliminated, enabling the observation of structured fluorescence excitation spectra and single vibronic level (SVL) fluorescence of cold, isolated anthracene.

In this paper we present a vibrational analysis of the fluorescence excitation spectrum of anthracene and the dispersed fluorescence spectra of jet-cooled h_{10}-; $9d_1$-; $9,10d_2$-; and d_{10}- anthracene. In addition, a study of rotational band contours in the h_{10}- anthracene excitation[7] spectrum is used as a guide for assigning certain bands of interest. For h_{10}- and d_{10}- anthracene, we compare our results with other experimental and theoretical results reported in the literature. Fluorescence results for the partially deuterated species have not appeared elsewhere.

In the accompanying papers[8,9] and others,[10] we make use of the data and assignments presented in this paper in the discussion of intramolecular vibrational energy redistribution (IVR) and quantum beats in anthracene, and intramolecular exiplex formation in an anthracene derivative. In addition, the work presented herein adds to the existing work on benzene,[11] naphthalene,[12] tetracene,[13] and pentacene,[14] and is, therefore, important to the understanding of the spectroscopy of this series of polyacenes.

II. EXPERIMENTAL

The complete details of the experimental apparatus will be deferred to subsequent publications[9,10] and, therefore, will only be outlined here. Two different jet setups were used; one with a continuous nozzle source[9] and the other pulsed.[10]

A. Continuous nozzle source

The continuous supersonic jet apparatus was used to obtain fluorescence excitation and dispersed fluorescence spectra. The free jet was created by passing an inert carrier gas (He, Ne, or N_2) over anthracene heated to 150–180 °C and expanding the gas through a 100 or 150 μm pinhole into a vacuum chamber at $< 10^{-3}$ Torr. The focused laser beam crossed the free jet at variable distances ($\equiv X$) of 3–5 mm from the pinhole. Fluorescence was collected with $f/1$ imaging optics, passed through a microprocessor-controlled monochromator (dispersion 16 Å/mm), and focused onto a photon counting photomultiplier tube. Data were acquired on a multichannel scalar prior to transfer to a PDP 11/23 computer for analysis. Vacuum corrections have not been made for the quoted absolute and relative frequencies.

Laser excitation for the dispersed fluorescence measurements was provided by a synchronously pumped, cavity-dumped picosecond dye laser. Output pulses were frequency doubled with a 1 cm thick $LiIO_3$ crystal. For some spectra the excitation bandwidth (FWHM) was 2 Å in the UV (dye laser tuning element: a two-plate birefringent filter), while other spectra correspond to excitation with 0.5 Å bandwidth excitation (three-plate birefringent filter and fine-tuning etalon as laser tuning elements). The spectral characteristics of the UV excitation were determined upon scattering the light into the monochromator. Monochromator calibration was performed using the output of a hollow cathode Fe–Ne lamp (this was not done simultaneously with the acquisition of anthracene spectra). Spectra were obtained for 0_0^0 excitation of all the anthracene species. In addition, dis-

[a] Present address: Bell Laboratories, 600 Mountain Avenue, Murray Hill, New Jersey 07974.
[b] IBM Research Fellow.
[c] Camille and Henry Dreyfus Foundation Teacher–Scholar.
[d] Contribution No. 6866.

 0021-9606/84/172195-14$02.10

persed fluorescence spectra were measured for excitation to various other single vibronic levels of h_{10}-anthracene in order to facilitate the assignment of excited state vibrational bands. Absolute and relative frequencies for the dispersed fluorescence spectra are quoted to ± 5 cm^{-1}.

Fluorescence excitation spectra were obtained using several experimental systems. In the first arrangement, the cavity-dumped laser source with a UV bandwidth of 2 Å was used. The front monochromator slit was opened to 1 mm and the rear slit assembly was removed to produce an effective detection bandwidth of 500 Å. The laser was tuned by means of a micrometer drive attached to the birefringent filter. The standard micrometer was replaced with a 2 in. micrometer head with ten-thousandths of an inch gradations in order to enable accurate and reproducible step adjustments. The laser was tuned in 0.4 Å increments and the wavelength in the UV was noted (using a Jarrell–Ash 0.5 m monochromator) every 15 steps in order to eliminate any major nonlinearity resulting from the tuning procedures. At each step, the phase matching angle of the lithium iodate frequency doubling crystal was adjusted to maximize the photon counting rate. Peak positions of the spectra were measured to be reproducible to within 0.4 Å. The resolution of the fluorescence excitation spectra was limited by the 2 Å laser bandwidth in the UV. Fluorescence excitation spectra taken in this way were not normalized to the laser power. In order to obtain high resolution, normalized fluorescence excitation spectra the procedures described in the following section were employed.

Fluorescence excitation spectra with the continuous nozzle source were also obtained using a frequency doubled (2 cm, angle-tuned KDP crystal), nitrogen laser-pumped scanning dye laser. The laser bandwidth was approximately 0.5 cm^{-1}. The absolute laser wavelength was calibrated using the optogalvanic method.[15] Although spectra were not normalized to UV power, they were found to be quite reproducible for a given set of experimental conditions and were found to match laser-normalized spectra (see below) for scans over a limited range.

B. The pulsed nozzle source

The combination of a pulsed nozzle source and the KDP-doubled output of a microprocessor controlled, scanning Nd-YAG pumped dye laser was used to obtain fluorescence excitation spectra normalized to laser pulse energy. The laser bandwidth in the UV was $\lesssim 0.5$ cm^{-1}. The pulsed jet was created by passing He, Ne, or N_2 over anthracene heated to 120–130 °C and expanding the gas through a solenoid controlled, 300 μm diameter opening into an evacuated chamber. The pressure of the vacuum chamber was typically $< 4 \times 10^{-4}$ Torr. The UV output of the laser, synchronized to the triggering of the pulsed nozzle, crossed the free jet 1.2 cm downstream from the expansion pinhole. The total fluorescence intensity was normalized to the PMT-detected UV pulse energy with a boxcar integrator. Relative intensities using this system were found to be quite reproducible. The absolute laser wavelength was calibrated using the optogalvanic method.[15] Frequencies are quoted to ± 2 cm^{-1} and are not corrected to vacuum.

C. Materials

H_{10}-anthracene (Aldrich) and d_{10}-anthracene (Aldrich) were zone refined (100 passes) prior to use. In addition, h_{10}-anthracene (Aldrich, $> 98\%$) was used without further purification. There was no apparent difference in observed results for purified vs unpurified anthracene. $9d_1$-anthracene and $9,10d_2$-anthracene were synthesized by acid-catalyzed deuterium–hydrogen exchange[16] from the respective precursors 9-bromoanthracene (Aldrich) and 9,10-bromoanthracene (Kodak). Purification was accomplished upon repeated recrystallization from $CHCl_3$. Isotopic purity was determined by mass spectral analysis to be $> 95\%$.

III. RESULTS AND DISCUSSION

A. Preliminaries

1. Molecular axis system and vibrational mode notation

In order to avoid confusion with regard to the designation of symmetry species, it is convenient at this point to define the molecular axis system to which we will refer. We use Pariser's notation.[17] This system defines the out-of-plane molecular symmetry axis as the z axis, the short, in-plane axis as the y axis, and the long, in-plane axis as the x axis. With this notation the S_1 state of anthracene (D_{2h} point group symmetry) is $^1B_{2u}^+$.[17] We note that most of the papers in the literature dealing with the vibrations of anthracene take the molecular axis system according to Mulliken's convention,[18] in which x is the out-of-plane axis and y is the long axis. The major consequence of this with regard to this paper is that b_{3g} vibrations in Mulliken's convention are of b_{1g} symmetry in the axis system we employ here.

In assigning vibrational bands, we shall employ the well-known notation used by Beck *et al.* and by others.[12] Totally symmetric modes are denoted by an integer; the highest energy mode being represented by a "1," and so on down to the lowest energy mode "12." Similarly, b_{1g} modes are represented by integers with bars over them (e.g., $\bar{1}$). A vibronic band involving m quanta of mode J in the excited state and n quanta of J in the ground state is denoted J_n^m. Combination bands are given as $J_n^m K_{n'}^{m'} \ldots$. Finally, excited state SVL's are conveniently represented in the form $J^m K^{m'} \ldots$.

2. Rotational constants and contour calculations

We have used a computer program to calculate the absorption rotational band contours of asymmetric top molecules. Details of the program can be found elsewhere.[19] Our use of the program is not to quantitatively fit observed band contours, but instead intended to distinguish (among) A-, B-, and C-type bands in the fluorescence excitation spectra in an effort to assign the symmetries of various vibronic transitions. We have made several assumptions in order to obtain the calculated results. Fluorescence excitation spectra are considered to be identical to absorption spectra. The rotational constants of anthracene, calculated to be 2155 MHz (x axis), 450 MHz (y axis), and 375 MHz (z axis) by reference to structural data,[20,21] are assumed to be independent of vi-

bronic level. Centrifugal distortion effects are assumed to be negligible. Finally, appropriate values for the rotational temperature of the free jet expansions were obtained by consideration of terminal translational temperatures.[20]

3. Vibronic symmetry

The S_1–S_0 electronic excitation in anthracene is short-axis polarized and corresponds to a ${}^1B_{2u}^+(\pi\pi^*)$–${}^1A_g^-$ transition.[4,22] Therefore, based on symmetry arguments, one expects only a_g, b_{1g}, and b_{3g} vibrational levels to be active in absorption from the S_0 vibrationless level and in emission from the S_1 vibrationless level. The nontotally symmetric b_g modes which are allowed by symmetry are forbidden by Franck–Condon considerations, but may gain intensity via vibronic coupling (Herzberg–Teller interaction) of the S_1 state with other electronic states. Since a ${}^1B_{3u}^+$ electronic state with a large oscillator strength for transitions to S_0 lies 13 600 cm^{-1} above S_1,[23] one might expect b_{1g} levels $(B_{3u} \times B_{2u})$ to gain significant intensity in $S_1 \leftrightarrow S_0$ spectra. In contrast, b_{3g} modes couple S_1 with ${}^1B_{1u}(\sigma\pi^*)$ electronic states, which are far removed in energy. As a result, one might not expect b_{3g} modes to figure prominently in S_1–S_0 spectra.

The above considerations with regard to vibrational activity have been taken into account in published work on anthracene spectroscopy. Based on experimental results using polarization techniques and oriented samples,[3,24] they have proved reliable. We follow this same reasoning here and analyze spectra primarily in terms of a_g and b_{1g} vibrational modes. Although $9d_1$-anthracene is of C_{2v} symmetry, the similarity of the d_1 spectra to the h_{10} spectra indicates that the d_1 results can also be analysed using D_{2h} symmetry considerations.

In anthracene, one expects 12 a_g modes. Three of these correspond to the C–H stretching vibrations which are not active in $\pi\pi^* \leftrightarrow S_0$ transitions. Thus, nine fundamentals are expected in the spectra reported here.

B. Vibrational cooling, van der Waal's complexes, and intermolecular interactions

While free jet spectroscopy presents enormous advantages, there are some problems that must be handled carefully. In particular, one must be aware that vibrationally hot molecules and/or weakly bound complexes may be present in the free jet expansion. An assessment of the contributions of both of these kinds of species to observed spectra can be made by means of an analysis of fluorescence excitation spectra as a function of carrier gas species and backing pressure. In Fig. 1 we present fluorescence excitation spectra taken with the pulsed-nozzle laser system in the region of the h_{10}-anthracene $S_1 \leftrightarrow S_0$ origin 3610.8 Å (27 695 cm^{-1}) for a variety of expansion conditions. Similar spectra are obtained using the continuous jet-nitrogen laser system. One notices the strikingly congestion-free spectra associated with N_2 as carrier gas compared to the He and Ne spectra. Based on the results and arguments of other groups,[7,25] one would expect N_2 to be a more efficient vibrational cooler than He or Ne, but at the same time to be more likely to form van der Waal's complexes. Thus, one might reasonably assign the weak features to the red of the origin in the N_2 spectrum as being due to van der Waal's species, while attributing the extra bands in the He and Ne spectra primarily to vibrationally hot molecules. Other results support this interpretation. For instance, we have found an increase in the relative intensity of the -41 cm^{-1} band in the N_2 spectra as the N_2 pressure is increased.[20] In addition, resolved fluorescence spectra corresponding to the excitation of -41 cm^{-1} and -63 cm^{-1} bands in the N_2 spectra reveal low frequency (30 cm^{-1}) intervals[20] which cannot be assigned to isolated anthracene ground state vibrations, but, instead, are likely to be associated with N_2-anthracene complexes. Regarding the spectra obtained with He and Ne it is telling that they are so similar. If any of the additional bands were due to complexes, one would expect to observe differences in the two excitation spectra. In addition, excitation of at least two of these bands (the ones appearing at -54 and -157 cm^{-1}) results in bands in the fluorescence spectra that occur to the blue of the excitation energy. This is proof that these excitation bands are due to vibrationally hot molecules.

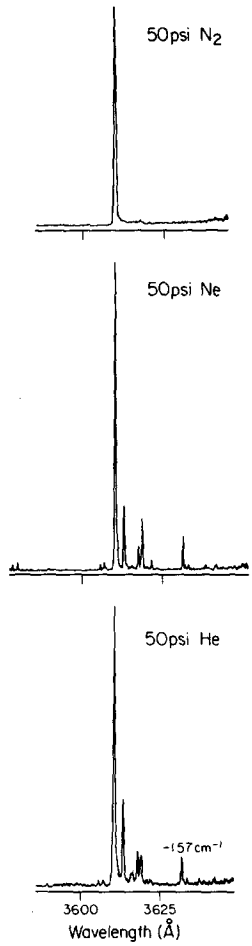

FIG. 1. Fluorescence excitation spectra about the 0_0^0 band (3610.8 Å, largest peak in all spectra) of h_{10}-anthracene as a function of carrier gas. Spectra were taken with the pulsed nozzle system (see the experimental section) and are normalized to laser pulse energy. To give an idea of the energy scale of the abscissa, the -157 cm^{-1} hot band is labeled in the helium spectrum.

Besides having to be cognizant of the possibility that various types of species might be present in the free-jet expansion, one must also be aware that collisional interactions

can give rise to spectroscopic manifestations. With nitrogen as carrier gas and upon excitation to levels other than 0^0, we have observed bands in dispersed fluorescence spectra which do not appear in He and Ne expansions. The bands decrease in relative intensity as X increases and give rise to long-lived fluorescence decays ($\sim$20 ns). These characteristics, along with the spectral positions of the bands, are consistent with emission arising from excited anthracene molecules that are collisionally relaxed to the vibrationless level of the excited states. Most of the dispersed fluorescence spectra presented in this paper were obtained for helium expansions to prevent such collisional effects.

In summary, we have found N_2 to be a better vibrational cooler than He and Ne, and also to have a greater propensity for intermolecular interaction. By correlating results taken with different carrier gases we are able to distinguish vibronic features which pertain to cold, isolated anthracene from those that pertain to vibrationally hot, collisionally relaxed, or van der Waal's species.

C. Assignment of S_0 vibrations

In Fig. 2 we present dispersed fluorescence spectra corresponding to excitation of the 0^0 levels of the four anthracene species. In addition, 0^0 spectra of h_{10}-anthracene, which have been limited to various intensity or wavelength ranges, are presented in Figs. 3(a) and 3(b). Finally, in Fig. 3(c) the 0^0 spectrum of d_{10}-anthracene is shown on an expanded intensity scale. Although spectra have not been corrected for any drift in laser power during the course of the scans, the relative intensities may be taken as reliable owing to the reproducibility of the spectra. Correction for the detection response of our system was not made. The contribution of scattered light to the intensity of the 0_0^0 bands was determined to be negligible. Band positions, relative intensities, and assignments for the spectra are given in Tables I–IV.

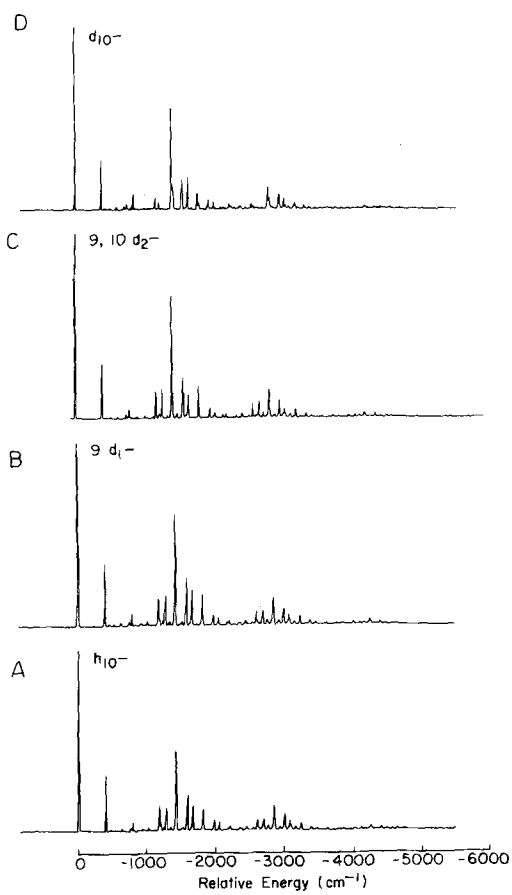

FIG. 2. 0^0-level fluorescence spectra of the various anthracene species. The energy scale is relative to the h_{10}-0_0^0 band. Experimental conditions: laser-to-nozzle distance (≡X) = 5 mm, sample temperature (≡T) = 150 °C, pinhole diameter (≡D) = 150 μm, carrier gas pressure (≡P) = 45 psi N_2, excitation bandwidth (≡BW) = 2 Å, monochromator resolution (≡R) ≃0.4 Å.

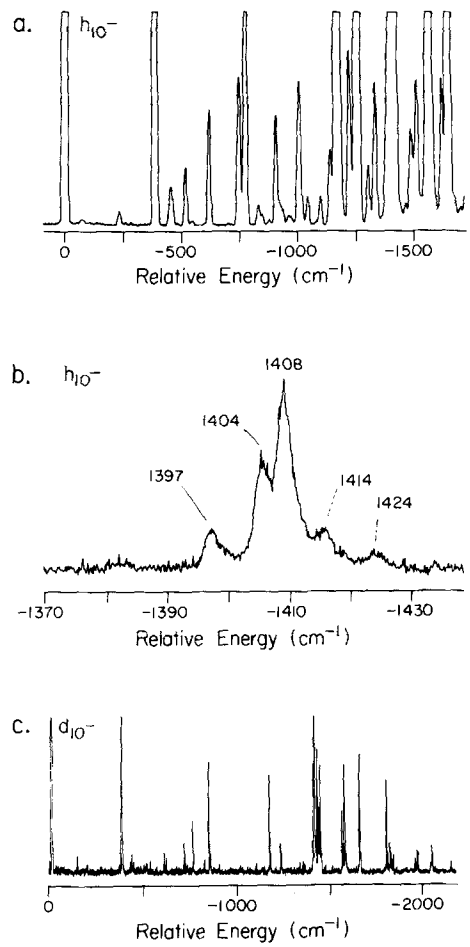

FIG. 3. (a) 0^0-level fluorescence of h_{10}-anthracene on a magnified intensity scale. X = 3 mm, D = 100 μm, P = 30 psi He, BW = 0.5 Å, R = 1.6 Å, T = 180 °C. The energy scale is relative to the excitation energy. (b) High resolution 0^0-level fluorescence of h_{10}-anthracene in the 1400 cm^{-1} region of the spectrum. The same conditions as (a) except R≃0.1 Å. (c) The 0^0 level, d_{10}-anthracene spectrum of Fig. 2(d) on a magnified intensity scale. Note the congestion in the 1400 cm^{-1} region.

1. S_0 vibrational assignments for h_{10}-anthracene

There exists a large body of literature dealing with the ground state vibrational structure of h_{10}-anthracene. By comparison with results from these studies we are able to identify nine a_g (1566, 1486, 1408, 1263, 1165, 1012, 753, 624, and 390 cm^{-1}) and six b_{1g} (1643, 1382, 1183, 1100, 912, and 524 cm^{-1}) fundamentals (see Table I) in the h_{10} spectra of Figs. 2 and 3. In making these assignments we have drawn from the results of Refs. 3, 5, and 24. Experimental values

TABLE I. 0^0-level fluorescence assignments for h_{10}-anthracene.

Shift (cm^{-1})	Intensity	Assignment	Exp. (Ref. 3)	Exp. (Ref. 5)	Exp. (Ref. 24)	Calc (Ref. 26)
0	100	27 695 cm^{-1} S_1 origin	...	...	...	...
237	1	b_{3g} fundamental?	...	...	242 (b_{2g})	...
390	45	$12_1^0(\overline{11}_1^0?)$	390	394	395	394
460	1	b_{3g} overtone?	...	...	...	...
524	1	$\overline{10}_1^0$	...	...	519	532
624	2	11_1^0	624	627	622	622
753	3	10_1^0	755	759	753	751
778	7	12_2^0	...	788	...	...
912	2	$\overline{9}_1^0$	...	...	901	907
1012	2	9_1^0	1007	1015	1007	1005
1050		...	...	...	...	...
1100	1	$\overline{8}_1^0$	...	...	1103	1112
1144	1	(753 + 390); (524 + 624)	...	...	...	...
1165	22	8_1^0	1162	1163	1163	1165
1183	3	$\overline{7}_1^0$	...	1185	1187	1184
1226	3	...	...	...	...	...
1250	4	...	...	...	...	...
1263	22	7_1^0	1257	1257	1260	1260
1304	1	(912 + 390)	...	...	...	...
1382	2	$\overline{5}_1^0$	1409?	1389	1376	1379
1397	9					
1404	30			1402		
1408	59	6_1^0-Fermi resonance	1402	1407	1403	1403
1414	9			1414		
1424	5			1426		
1486	2	5_1^0	...	...	1482	1482
1519	2	...	...	...	...	...
1531	1	...	...	...	...	...
1555	7	(390 + 1165)	...	(394 + 1163)	...	...
1566	31	4_1^0	1559?	1566	1557	1557
1643	20	$\overline{3}_1^0$	...	1639	1634	1626
1654	3	(390 + 1263)	...	(394 + 1268)	...	...
1785	10	390 + 1397	...	...	...	...
1797	16	390 + 1408	...	(394 + 1402) (394 + 1407)	...	...

from these studies, along with calculated values,[26] are included in Table I.

The assignments of the a_g modes agree well with both Raman work[24] and calculated results.[26] The dominance of the "6" (1408 cm^{-1}) and "12" (390 cm^{-1}) modes, as well as the general appearance of the spectrum, is similar to that which is observed in low temperature matrix experiments.[3-5] We note the presence in our spectrum of the fundamental of the "5" mode (1486 cm^{-1}), which is prominent in Raman spectra[24] but which has not previously been observed in luminescence spectra. Just as in condensed phase work,[5] we observe several bands of significant intensity in the region of the 6_1^0 band [Fig. 3(b)], indicating the existence of vibrational mixing in the 1400 cm^{-1} region of the S_0 vibrational level structure. At least two combination bands involving a_g modes, $9_1^0 12_1^0$(1402 cm^{-1}) and $11_1^0 12_2^0$(1404 cm^{-1}), might be expected to gain significant intensity via Fermi resonance interactions involving the 6_1 vibrational level.

The b_{1g} mode assignments also agree well with other work. Several points may be noted. Firstly, there is no evidence to indicate the presence of a b_{1g} fundamental at ~390 cm^{-1} ($\overline{11}_1^0$), although Raman work[24] suggests that such a fundamental does exist. Our inability to see such a band, even at better than 1 cm^{-1} resolution, is probably due to its overlap with the intense 12_1^0 band, with its rotational width of several cm^{-1}. Secondly, we have assigned the 1382 cm^{-1} band as $\overline{5}_1^0$ to agree with Raman assignments[24] and calculated frequencies.[26] It is conceivable that, instead, the 1397 cm^{-1} band might be this fundamental. Finally, all the b_{1g} fundamentals observed, except the $\overline{3}_1^0$ band, are fairly weak

in intensity. Being that their intensities are derived from vibronic coupling interactions, this is not surprising.

Several bands occur in the 0^0 level fluorescence spectrum that cannot be assigned to a_g or b_{1g} fundamentals or combination bands. In particular, one may notice the bands at 237 and 460 cm^{-1} [see Fig. 3(a)]. The 237 cm^{-1} band has been observed in Raman spectra (242 cm^{-1}) and has been tentatively assigned as b_{2g}.[24] In light of the fact that we observe it in fluorescence, the band probably represents, instead, the fundamental of the lowest energy b_{3g} mode. The 460 cm^{-1} band is then assigned as the first overtone of this mode. The fact that this implies a fairly anharmonic vibration is not particularly troublesome, being that the vibrational motion is out of plane. It will be shown below that there are excited state counterparts to these ground state intervals.

2. S_0 assignments for $9d_1$- and $9,10d_2$-anthracene

By direct analogy to the h_{10}-anthracene fluorescence spectrum, the assignment of the d_1-anthracene spectrum can be accomplished without invoking the effects of isotopic induced mode scrambling recently discussed.[27] Doing so, one obtains the assignments presented in Table II. Again, nine a_g fundamentals are assigned. Five b_{1g} modes are also assigned; we are not, however, able to observe a band corresponding to the b_{1g}-assigned 1100 cm^{-1} band that is weakly present in the h_{10} spectrum. As is evident in Table II, any monodeuteration shifts of vibrational frequencies relative to anthracene are small. Furthermore, it appears that the reduction of symmetry to C_{2v} does not have any major effect on the optical activity of the modes. The shift of the $9d_1$-anthracene 0_0^0 energy relative to that of h_{10}-anthracene is + 14 cm^{-1}, a value quite reasonable considering the isotope shifts of other aromatics.

TABLE II. 0^0-level fluorescence assignments for $9d_1$-anthracene.

Shift (cm^{-1})	Intensity	Assignment
0	100	Origin 27 709 cm^{-1}
390	32	12_1^0
457	2	b_{3g} overtone?
517	2	$\overline{10}_1^0$
626	3	11_1^0
734	2	...
750	3	10_1^0
784	7	12_2^0
902	3	$\bar{9}_1^0$
1015	4	9_1^0
1141	2	(750 + 390)
1166	16	8_1^0
1182	5	$\bar{7}_1^0$
1226	3	...
1251	4	...
1261	18	7_1^0
1271	4	$\bar{6}_1^0$?
1293	2	...
1339	3	...
1374	2	$\bar{5}_1^0$
1396	5	...
1410	67	6_1^0
1426	4	...
1482	4	5_1^0
1497	3	...
1557	12	(1166 + 390)
1567	30	4_1^0
1639	18	$\bar{3}_1^0$
1649	9	(1261 + 390)
1799	18	(1410 + 390)
1957	8	(1567 + 390)
2032	6	(1639 + 390)

TABLE III. 0^0-level fluorescence assignments for 9, 10 d_2-anthracene.

Shift (cm^{-1})	Intensity	Assignment	Calc (Ref. 21)
0	100	Origin 27 714 cm^{-1}	...
390	35	12_1^0	395
507	2	$\overline{10}_1^0$	500
617	3	11_1^0	640
706	2	...	...
741	4	10_1^0	745
779	8	12_2^0	...
804	2	...	...
849	2	...	...
867	2	...	...
890	3	$\bar{9}_1^0$	855
1011	4	9_1^0	1005
1164	13	8_1^0	1150
1224	3	...	...
1249	4	...	...
1262	14	7_1^0	1250
1337	3	...	...
1374	3	$\bar{5}_1^0$	1385
1402	56	6_1^0	1397
1414	5	Fermi resonance?	
1421	3		
1481	4	5_1^0	1480
1546	3	...	
1556	9	(390 + 1164)	...
1564	19	4_1^0	1557
1607	3	...	...
1628	4	...	...
1640	8	$\bar{3}_1^0$	1629
1647	4	(1262 + 390)	...
1796	13	(1402 + 390)	...
1812	1	(1414 + 390)	...
1879	3	...	...
1946	4	(1164 + 2×390)	...
1955	7	(1564 + 390)	...
2027	3	(1640 + 390)	...

The same criteria used to assign the d_1 spectrum are applicable to the analysis of the d_2-anthracene spectrum [Fig. 2(c)]. The results are given in Table III along with calculated frequencies[28] from the literature. For d_2-anthracene, the 0_0^0 isotope shift is + 19 cm^{-1}.

3. S_0 assignments for d_{10}-anthracene

Comparison of Fig. 2(d) with Figs. 2(a)–2(c) reveals that perdeuteration results in some noticeable changes in the dispersed fluorescence of d_{10}-anthracene relative to the other species. Clearly, many features are common to all the spectra and this has led us to many of the assignments appearing in Table IV. However, the relatively strong bands at 843 and 1165 cm^{-1} represent bands undergoing large deuteration shifts. Following the assignments of Ref. 5 and the calculated results of Ref. 26, we assign these as the 8_1^0 and 7_1^0 bands,

TABLE IV. 0^0-level fluorescence assignments for d_{10}-anthracene.

Shift (cm^{-1})	Intensity	Assignment	Exp. (Ref. 3)	Calc. (Ref. 26)
0	100	Origin 27 770 cm^{-1}	...	...
378	31	12_1^0	376	380
528	1	$\overline{10}_1^0$?	...	501
603	1	11_1^0	594	602
711	1	10_1^0	709	702
755	6	12_2^0	...	...
817	2	$\overline{9}_1^0$?	...	804
843	12	8_1^0	839[a] 835	834
850	2	9_1^0?	...	824
891	2	$\overline{8}_1^0$?	...	865
1090	1	(711 + 378)	...	...
1165	10	7_1^0	1162[a] 1154	1164
1222	4	843 + 378	...	...
1382	4	...	...	...
1390	46	...	1382	6_1^0 1376
1405	14	6_1^0	1401	5_1^0 1431
1414	10	Fermi resonance		
1421	13	and 5_1^0?		
1483	2	...	...	...
1533	9	...	...	...
1545	16	4_1^0, $\overline{4}_1^0$,	4_0^1, 1528	4_0^1, 1526
1548	10	(1165 + 378)		$\overline{4}_0^1$, 1550
1624	17	$\overline{3}_1^0$	...	1585
1765	13	(1390 + 378)	...	...
1782	5	(1405 + 378)	...	...
1788	3	(1414 + 378)	...	...
1797	3	(1421 + 378)	...	...
1910	3	(1165 + 378)		
1922	4	(1546 + 378)		
1997	5	(1624 + 378)		

[a] Reference 5.

respectively (corresponding to h_{10} values of 1165 and 1263 cm^{-1}, respectively). The 9_1^0, $\overline{9}_1^0$, and $\overline{8}_1^0$ transitions (h_{10} values of 1012, 912, and 1100 cm^{-1}) could conceivably be associated with the bands observed at 817, 843, and 892 cm^{-1} in the d_{10} spectrum. The assignments for these bands have been made strictly by reference to Ohno's calculations.[26] The spectral congestion in the 1400 cm^{-1} region [Fig. 3(c)] precludes any definite assignment of an analog to the h_{10}, 5_1^0 band (1486 cm^{-1}). Calculations[26] suggest that any one of the bands at 1405, 1414, or 1421 cm^{-1} could correspond to this mode. It is notable that, just as for h_{10}-anthracene, there are a number of significantly intense bands within several cm^{-1} of the 6_1^0 band. Again, this is indicative of vibration–vibration interaction in the 1400 cm^{-1} region of the S_0 vibrational level structure. Finally, we note that the deuteration shift of the 0_0^0 energy is + 75 cm^{-1} for d_{10} relative to h_{10}-anthracene. This value is only accurate to ± 10 cm^{-1} because of the low resolution excitation spectrum taken for d_{10} (Fig. 5).

D. Assignment of S_1 vibrations of h_{10}-anthracene

Normalized excitation spectra of jet-cooled h_{10}-anthracene in N_2 and He expansions are presented in Fig. 4. Spectra of similar quality are not available for the deuterated species, however, spectra taken using the cavity-dumped laser system are shown in Fig. 5. For comparison with Fig. 4, we

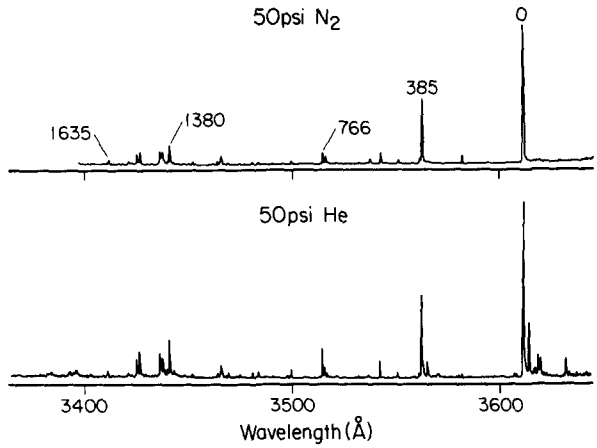

FIG. 4. Normalized fluorescence excitation spectra of h_{10}-anthracene taken with the pulsed nozzle system. Carrier gas parameters are given in the figure. Other conditions are given in the text. Various bands are labeled in the N_2 spectrum to give an idea of the energy scale.

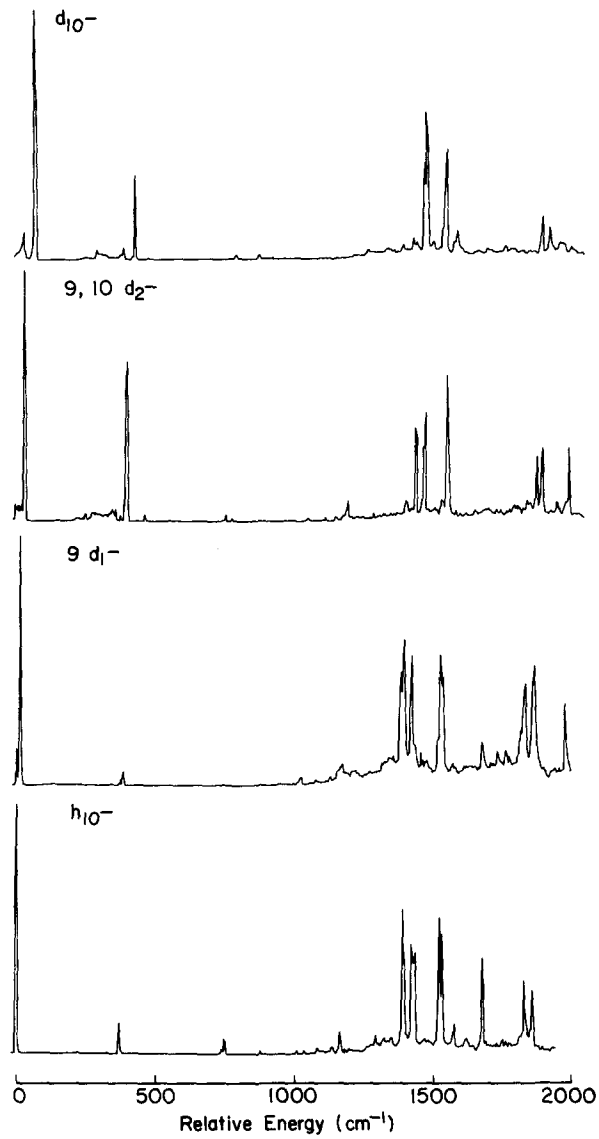

FIG. 5. Fluorescence excitation spectra of the various anthracene species taken with the cavity-dumped laser and cw jet. Spectra are not normalized to laser pulse energy. The energy scale is relative to the 0_0^0 energy of h_{10}-anthracene. The weaker bands to the red of the 0_0^0 bands in the spectra of deuterated species are probably due to isotopic impurities. For all spectra: X = 5 mm, D = 150 μm, P = 45 psi N_2, T = 150 °C. Other experimental details appear in the text.

TABLE V. h_{10}-anthracene excitation spectrum assignments.

Shift	Intensity	Assignment	Exp. (Ref. 3)	S_0 Values (Table I)
0	100	Origin 27 695 cm^{-1}		
209	1	b_{3g} fundamental?		237
232	3	$\overline{11}_0^1$		391[a]
385	31	12_0^1	385	390
395	1	b_{3g} overtone?		460
473	2	$\overline{10}_0^1$		524
541	5	$\overline{11}_0^2$		
583	2	11_0^1	589	624
748	1	...		
755	4	10_0^1	737	753
766	8	12_0^2		
889	2	$\overline{9}_0^1$		912
1019	2	9_0^1	1024	1012
1042	1	...		
1094	1	...		
1168	5	8_0^1 or 7_0^1	1155	1165 or 1263
1184	1	$\overline{7}_0^1$	...	1183
1291	1	...		
1380	12	6_0^1	1389	1408
1389	2	...		...
1409	7	$b_{1g}(\overline{5}_0^1)$		1382
1420	7	$a_g(5_0^1)$		1486
1501	10	$a_g(4_0^1)$	1496	1566
1514	6	$b_{1g}(\overline{4}_0^1)$		1576[a]
1550	2	(1168 + 385)		
1635	2	$\overline{3}_0^1$?		1643
1767	2	(1380 + 385)		
1792	3	(1409 + 385)		
1801	2	(1420 + 385)		

[a] Reference 24 (Raman).

include in Fig. 5 a spectrum of h_{10}-anthracene taken using the cavity-dumped laser. It is apparent that the relative intensities of bands appearing in the spectra shown in Fig. 5 are not very indicative of the actual situation and, therefore, we will not present an analysis of these spectra. They are included for the sake of completeness and for future reference. Band positions, intensities, and assignments for the upper spectrum presented in Fig. 4 are included in Table V. The following sections are devoted to a discussion of the assignments of bands in this spectrum.

1. Assignment of excited state vibrations

We have used various criteria in the assignment of the excitation spectrum of h_{10}-anthracene (Fig. 4). Some assignments have been made by others and appear in the literature. We have drawn particularly from the mixed crystal absorption work of Ref. 3. Pertinent values from this work appear in Table V. In addition, we have relied on correlation with ground state vibrational modes. Most useful in this regard has been the analysis of dispersed fluorescence spectra taken for the excitation of specific bands in the excitation spectrum. If a SVL of the form J^1 is excited, then in the absence of significant vibrational level interactions, one generally expects the J_1^1 band to act as a false origin for a 0^0-like fluorescence spectrum. This fact can be used to determine the

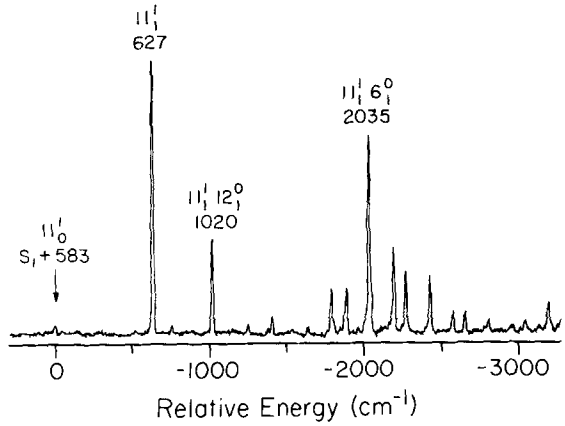

FIG. 6. Dispersed fluorescence spectrum of h_{10}-anthracene excited to $S_1 + 583\ cm^{-1}$. The arrow marks the spectral position of the excitation energy. The energy scale is relative to the excitation energy. X = 3 mm, D = 100 μm, P = 30 psi He, BW = 0.5 Å, R = 1.6 Å, T = 180 °C.

ground state value of the J fundamental. If this S_0 value corresponds to an assigned vibration, then the identify of J can be assigned. For example, Fig. 6 shows the fluorescence spectrum that results upon excitation to the band at $S_1 + 583\ cm^{-1}$. The spectrum appears similar to the 0^0 level fluorescence spectrum but with an intense origin that occurs at a shift of 627 cm^{-1} from the excitation energy. This shift corresponds to the value previously assigned to the ground state "11" mode (624 cm^{-1}, Table I). One, therefore, assigns the $S_1 + 583\ cm^{-1}$ band to the 11_0^1 transition. As will be discussed below, similar methods have been used to assign many of the bands appearing in Fig. 4. As an additional method used for the assignment of some excited state bands, we have measured and analyzed rotational band contours. These results, which primarily serve to facilitate the assignment of bands at energies greater than $S_1 + \sim 1300\ cm^{-1}$, will be presented and discussed after we have dealt with the bands which could be assigned by reference to dispersed fluorescence spectra.

2. Low energy a_g assignments

The assignment of many of the low energy a_g excited state modes is accomplished by using dispersed fluorescence spectra. Figures 6–10 show the SVL fluorescence spectra

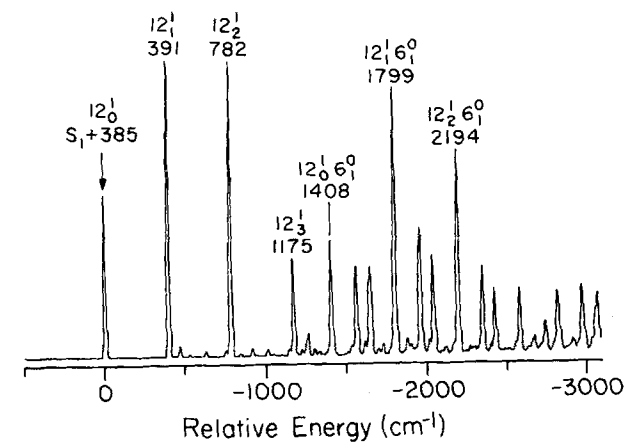

FIG. 7. Dispersed fluorescence spectrum of h_{10}-anthracene excited to $S_1 + 385\ cm^{-1}$. All notation and conditions are the same as for Fig. 6.

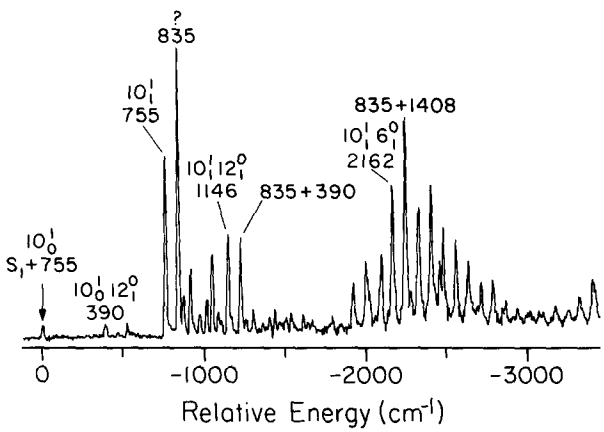

FIG. 8. Dispersed fluorescence spectrum of h_{10}-anthracene excited to $S_1 + 755$ cm^{-1}. The notation and experimental conditions are the same as for Fig. 6.

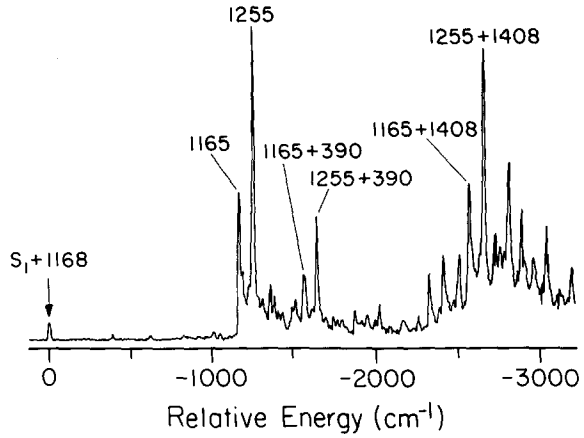

FIG. 10. Dispersed fluorescence spectrum of h_{10}-anthracene excited to $S_1 + 1168$ cm^{-1}. The notation and experimental conditions are the same as for Fig. 6.

corresponding to excitation of the low energy bands assigned as excited state a_g fundamentals (385, 583, 755, 1019, and 1168 cm^{-1}). Assigned bands and energy shifts are noted in the figures. The assignments for the 385(12_0^1), 583(11_0^1), and 1019 cm^{-1} (9_0^1) excited state fundamentals are easily made from the spectra, as is the assignment of the 766 cm^{-1} band as 12_0^2 (see Fig. 11). Comparing Fig. 8 to Fig. 12 ($S_1 + 748$ cm^{-1}) shows that the assignment of the 10_0^1 band is not quite so obvious, since the 753 cm^{-1} ground state interval appears prominently in both spectra. The assignment of 755 cm^{-1} as 10_0^1 is made on the basis of its greater intensity in the excitation spectrum. It seems likely that the 748 cm^{-1} band gains its intensity through excited state vibration–vibration coupling involving the 10^1 level. The 1168 cm^{-1} band assignment is not unambiguous since both the 8 and 7 fundamentals appear prominently in the dispersed fluorescence spectrum (Fig. 10). Assigning it as 8_0^1 would yield an excited state fluorescence value similar to the S_0 value. However, the 1255 cm^{-1} interval is very strong in the spectrum. In Table V both 8_0^1 and 7_0^1 are included as being possible assignments for the 1168 cm^{-1} band. Although the excited state band at 1291 cm^{-1} appears to be a likely candidate for the 7_0^1 band, its SVL spectrum (not shown) does not exhibit a 7_1^1 false origin.

The reader may note that other bands have been assigned as a_g fundamentals in Table V. These assignments have been made primarily on the basis of the rotational band contour results to be discussed later.

3. Low energy b_{1g} assignments

In Figs. 13–16 SVL spectra are presented which correspond to excitation of low energy bands assigned to excited state b_{1g} fundamentals. Based on the spectra presented in Figs. 14 and 15, the assignments of the 473 and 889 cm^{-1} bands as $\overline{10}_1^0$ and $\overline{9}_1^1$, respectively, are readily made. The 1184 cm^{-1} band could possibly be assigned as the fundamental of the $\overline{7}$ mode given the appearance of the 1183 cm^{-1} ground state interval in the SVL spectrum of Fig. 16. Analysis of this spectrum, however, is not straightforward.

The assignment of the 232 cm^{-1} band as the $\overline{11}$ fundamental (S_0 value of 390 cm^{-1} from Raman work[24]) is made somewhat tentatively since such an assignment implies a very large frequency shift between vibrational frequencies in the S_1 and S_0 states. Reasons for making the assignment as we have done may be found in the SVL spectrum of Fig. 13.

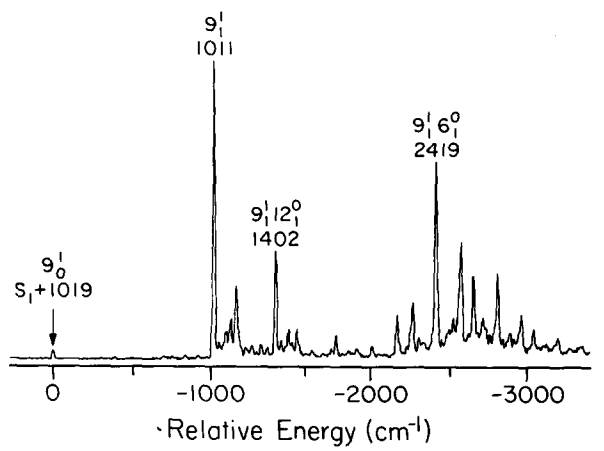

FIG. 9. Dispersed fluorescence spectrum of h_{10}-anthracene excited to $S_1 + 1019$ cm^{-1}. The notation and experimental conditions are the same as for Fig. 6.

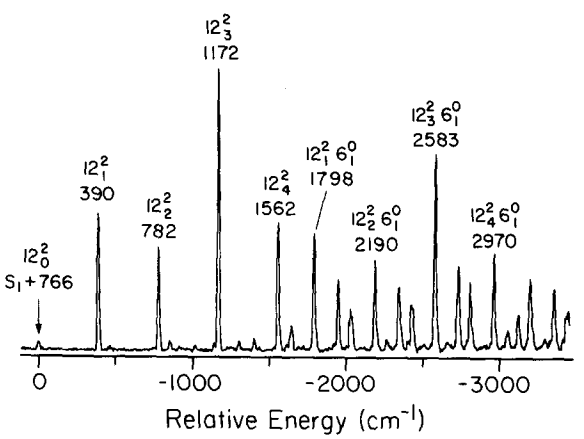

FIG. 11. Dispersed fluorescence spectrum of h_{10}-anthracene excited to $S_1 + 766$ cm^{-1}. The notation and experimental conditions are the same as for Fig. 6.

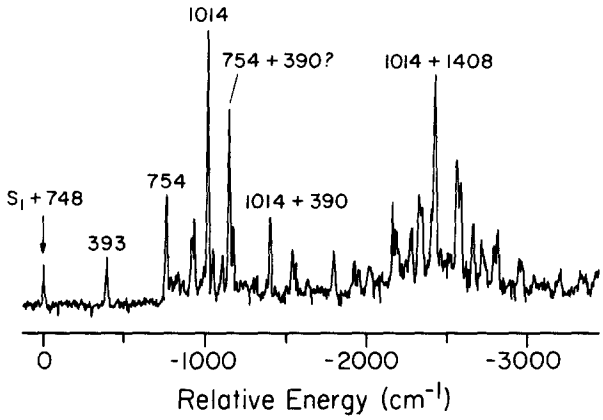

FIG. 12. Dispersed fluorescence spectrum of h_{10}-anthracene excited to $S_1 + 748\ cm^{-1}$. The notation and experimental conditions are the same as for Fig. 6.

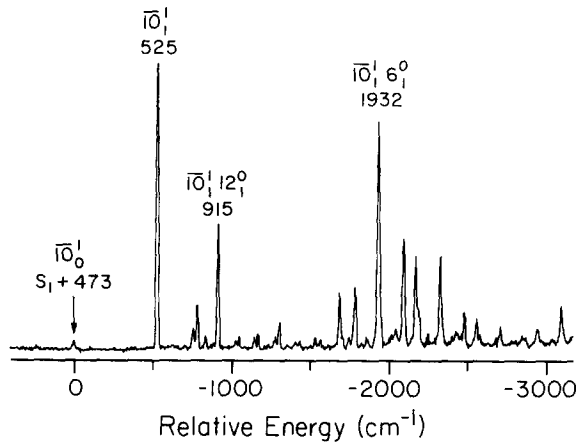

FIG. 14. Dispersed fluorescence spectrum of h_{10}-anthracene excited to $S_1 + 473\ cm^{-1}$. The notation and experimental conditions are the same as for Fig. 6.

Not only does the band at 391 cm^{-1} have the characteristics of a J^1_1-type band, but, also, the $\overline{10}$ fundamental appears prominently in the spectrum. This last fact would be expected only for an excited state vibrational level of b_{1g} symmetry. Further evidence for the association of the 232 cm^{-1} band with a ground state vibrational level at 390 cm^{-1} may be taken from Fig. 17. This spectrum was obtained for excitation of the vibrational hot band at $-157\ cm^{-1}$. Clearly the level that is excited is identical with the $S_1 + 232\ cm^{-1}$ level. This confirms the assignment of Ref. 7, in which the -157 cm^{-1} band is taken as the transition $S_1 + 232$ $cm^{-1} \leftarrow S_0 + 390\ cm^{-1}$. That this band is so much more intense than the $S_1 + 232\ cm^{-1} \leftarrow S_0 + 0\ cm^{-1}$ transition implies that the hot band is a J^1_1-type transition involving a nontotally symmetric mode (i.e., $\overline{11}$).

The emission spectrum of the SVL populated by excitation to $S_1 + 541\ cm^{-1}$ is very similar to that of the SVL assigned as $\overline{11}^1$, as may be seen by comparison of Fig. 18 with Figs. 13 and 17. Because of this and the fact that the most prominent band in the spectrum of Fig. 18 occurs at a shift of 778 cm^{-1} from the excitation energy, we assign the $S_1 + 541\ cm^{-1}$ transition as $\overline{11}^2_0$. All of the remaining intense bands in the spectrum may then be assigned as overtones or combination bands involving no net change in b_{1g} quantum numbers (i.e., $\overline{11}^2_2$, $\overline{11}^2_0\ \overline{10}^0_2$, etc.). It is noteworthy that weak bands assignable as $\overline{11}^2_1$ and $\overline{11}^2_0\ \overline{10}^0_1$ are also observed.

The assignment of the 232 and 541 cm^{-1} excitation spectrum bands as $\overline{11}^1_0$ and $\overline{11}^2_0$, respectively, implies that there is an interaction that greatly perturbs the excited state $\overline{11}$ mode. One possible interaction is strong vibronic coupling with one or both of the $^1B_{3u}$ electronic states[17] lying fairly close at higher energies. Such coupling would tend to distort the potential surface associated with the mode and, thus, give rise to irregular vibrational spacings. In this regard, it is interesting that the 232 and 541 cm^{-1} bands were not reported by Small in his mixed crystal absorption study,[3] despite the significant intensity with which they appear in the spectra of Fig. 4. In a vibronic coupling scheme this could be explained in terms of a reduction in coupling strength resulting from matrix induced perturbations.

The b_{1g} assignments of higher energy bands (Table V) will be considered in the rotational band contour discussion.

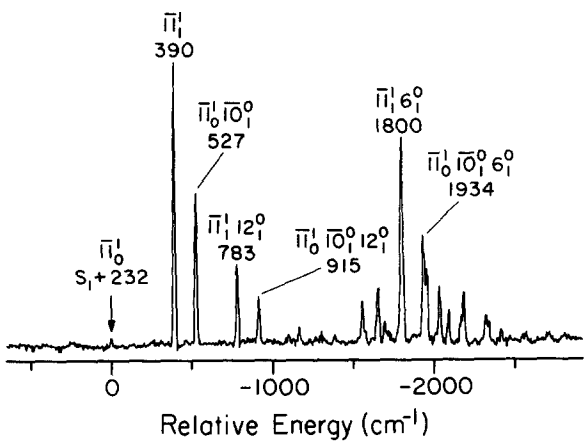

FIG. 13. Dispersed fluorescence spectrum of h_{10}-anthracene excited to $S_1 + 232\ cm^{-1}$. The notation and experimental conditions are the same as for Fig. 6.

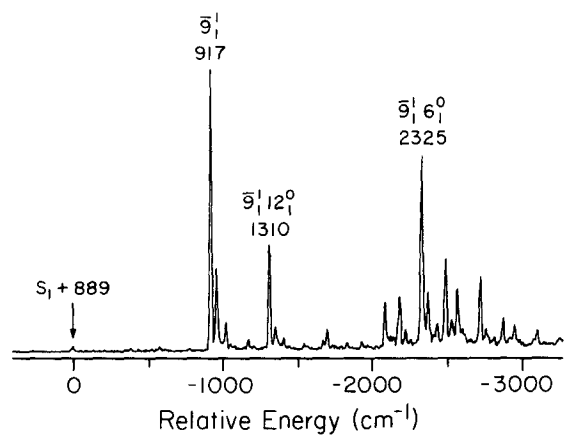

FIG. 15. Dispersed fluorescence spectrum of h_{10}-anthracene excited to $S_1 + 889\ cm^{-1}$. The notation and experimental conditions are the same as for Fig. 6.

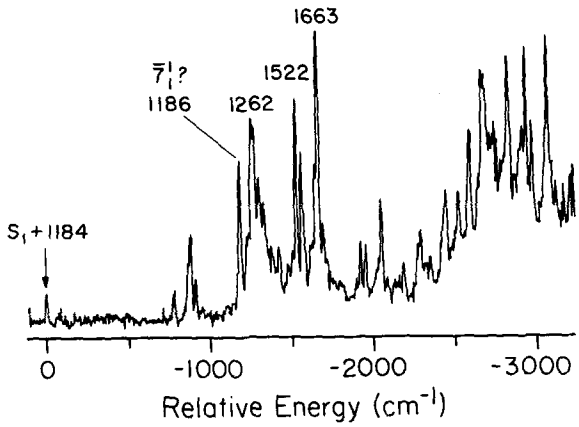

FIG. 16. Dispersed fluorescence spectrum of h_{10}-anthracene excited to $S_1 + 1184\,cm^{-1}$. The notation and experimental conditions are the same as for Fig. 6.

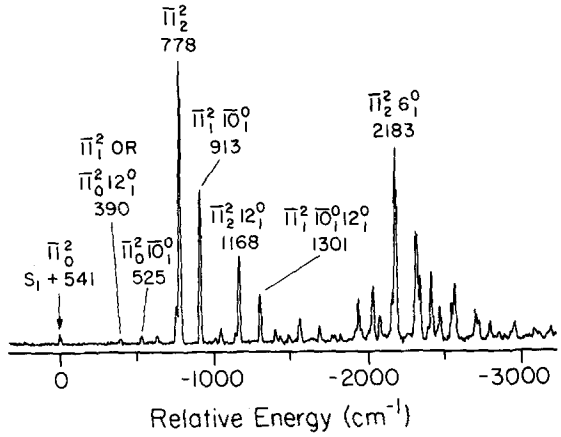

FIG. 18. Dispersed fluorescence of h_{10}-anthracene excited to $S_1 + 541$ cm^{-1}. The notation and experimental conditions are the same as for Fig. 6.

4. The 209 and 395 cm^{-1} bands

Dispersed fluorescence spectra which result upon excitation of the weak 209 and 395 cm^{-1} bands appearing in the h_{10}-anthracene excitation spectrum are presented in Fig. 19. From these spectra, it appears that the excited state SVL's corresponding to these bands are linked with the S_0 levels at 237 and 460 cm^{-1}, respectively. If one accepts the assignment of the ground state values as the fundamental and overtone of the lowest energy, b_{3g} vibrational mode, then analogous S_1 assignments may be made for the 209 and 395 cm^{-1} excitation spectrum bands. We note that Hays *et al.*[7] have suggested that the 209 and 395 cm^{-1} bands could represent the fundamental and overtone of a very anharmonic vibration.

5. Rotational contours: 0_0^0 and high energy bands

The assignment of those bands in Fig. 4 that occur at energies $\gtrsim S_1 + 1300\,cm^{-1}$ cannot be readily made solely by reference to SVL fluorescence spectra. This is because these spectra are congested[8] and the straightforward assignment of dispersed fluorescence features is not, in general, possible.

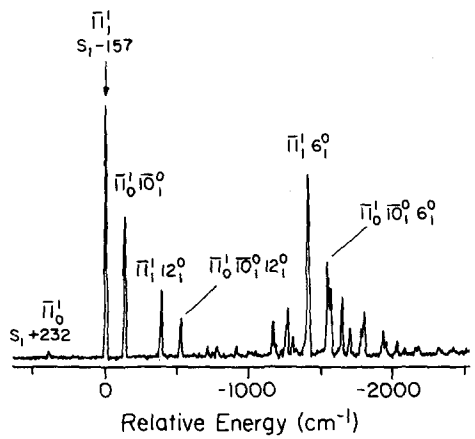

FIG. 17. Dispersed fluorescence spectrum of h_{10}-anthracene excited to the hot band at $S_1(0_0^0)$ - 157 cm^{-1}. The notation and experimental conditions are the same as for Fig. 6. Note the band at + 390 cm^{-1} (S_1 + 232 cm^{-1}) to the blue of the excitation energy. Compare this spectrum with that of Fig. 13.

Therefore, in order to facilitate the assignment of several bands in Fig. 4 we have obtained excitation spectra over their rotational contours. Figure 20 shows a series of spectra obtained for the 0_0^0 band using different expansion conditions. (Similar spectra were obtained for the 385 cm^{-1} (12_0^1) band.) This band is expected to be *B*-type, owing to the short-axis polarization of the $^1B_{2u}^+ \leftarrow {}^1A_g^-$ transition moment. Figure 21 displays calculated band contours (see Sec. III A.1) of a *B*-type band for various rotational temperatures. While no attempt has been made to optimize the large number of parameters involved in the calculations and, thus, to fit the

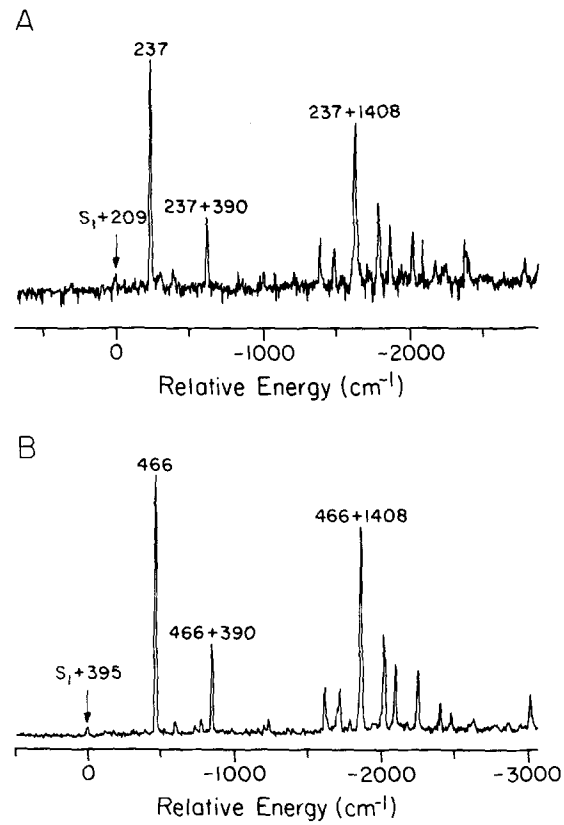

FIG. 19. Dispersed fluorescence spectra of h_{10}-anthracene excited to (a) $S_1 + 209\,cm^{-1}$ and (b) $S_1 + 395\,cm^{-1}$. The notation and experimental conditions are the same as for Fig. 6.

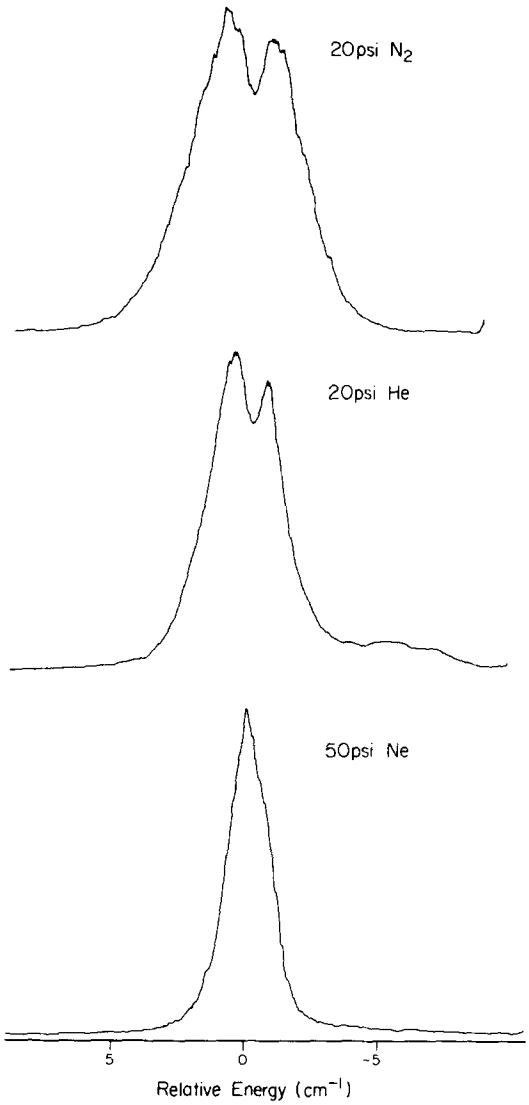

FIG. 20. Normalized fluorescence excitation spectra taken with the pulsed nozzle system over the 0_0^0 band of h_{10}-anthracene under different carrier gas conditions.

experimental band contours, the trends displayed in Fig. 21 clearly match those of Fig. 20. The contours of the 0_0^0 band then, are consistent with *B*-type rotational band contours for

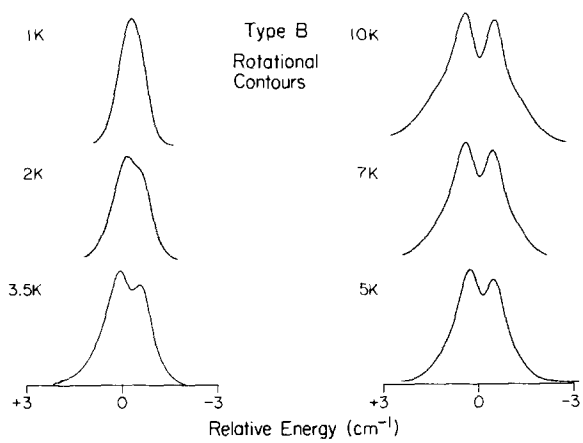

FIG. 21. Calculated (see the text) *B*-type rotational contours of anthracene as a function of rotational temperature.

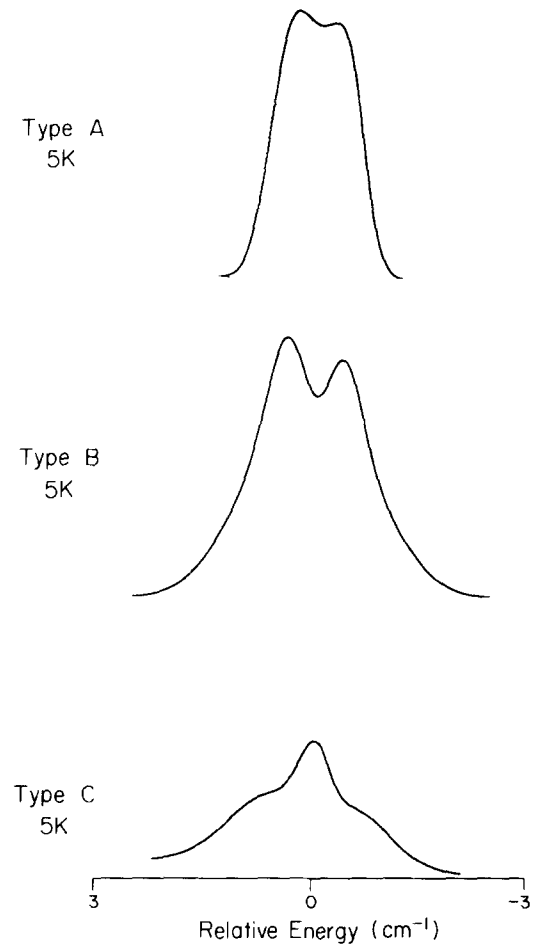

FIG. 22. A comparison of calculated *A*-, *B*-, and *C*-type absorption rotational contours for anthracene at a rotational temperature of 5 K. Note the pronounced splitting of the *B*-type band relative to the other two types.

different rotational temperatures; i.e., $T(\mathrm{Ne}) \lesssim T(\mathrm{He}) < T(\mathrm{N_2})$. This trend matches expectations derived from consideration of the calculated terminal translational temperatures of the different expansions.[20] In contrast to *B*-type contours, calculated *A*- and *C*-type contours match the general appearance of the 0_0^0 band much less well. These calculated contours are shown in Fig. 22 for a rotational temperature of 5 K.

The very noticeable differences in the types of rotational band contours for anthracene can be used as a basis to assign excitation bands. Transitions to $S_1\, a_g$ vibrational levels will be *B*-type and those to b_{1g} will be *A*-type. Reference to Fig. 22 shows that *B*-type contours are expected to exhibit much more pronounced band splittings than *A*-type contours for a given set of expansion conditions. Hence, based upon a comparison of the splittings for different bands, one can assign the symmetries of S_1 vibrational levels. Figure 23 shows excitation spectra of anthracene taken in the 1350–1550 cm^{-1} region for expansions utilizing 50 psi Ne and 5 psi N_2.

Comparison of the two spectra shows that all bands broaden in going from Ne to N_2, a trend consistent with the temperature trend derived from the 0_0^0 band. Furthermore, several prominent bands (those which appear at 1380—see

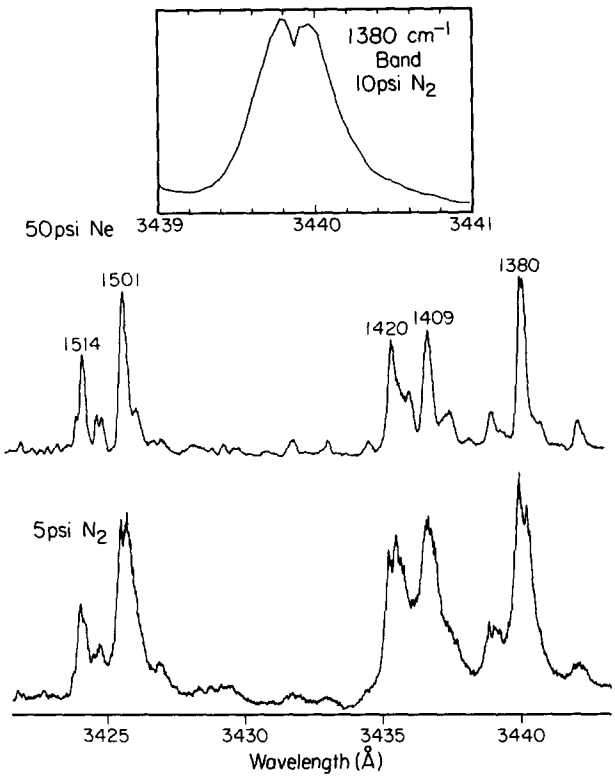

FIG. 23. Fluorescence excitation spectra of h_{10}-anthracene in the $S_1 + 1350$ to $S_1 + 1550$ cm^{-1} region for different carrier gas conditions. The spectra were taken with the pulsed nozzle system and are normalized. Prominent bands are labeled in the neon spectrum. Besides the general broadening of the spectrum, note the splitting of the 1380, 1420, and 1501 cm^{-1} bands when the carrier gas changes from 50 psi Ne to 5 psi N_2. The splitting of the 1380 cm^{-1} band is apparent in the inset of the figure.

inset of Fig. 23—1420, and 1501 cm^{-1}) are split in the N_2 spectrum, while other bands (most notably those at 1409 and 1514 cm^{-1}) remain unsplit. We assign the split bands to a_g vibrational levels and the unsplit bands to b_{1g} levels. The specific mode assignments that appear in Table V regarding these bands are made on the basis of spectral position and intensity. For instance, *the* 1380 cm^{-1} *band*, because of its intensity and its frequency, is taken to correspond to the excited state fundamental of the strongly optically active "6" mode, having a ground state analog at 1408 cm^{-1}. In making these assignments we have assumed that the most intense bands in Fig. 23 correspond to fundamentals. Of course, it is always possible that combination bands gaining their strength through, e.g., Fermi resonance, could appear prominently in the excitation spectra. It is for this reason that we have placed some specific mode assignments in parentheses in Table V, as an indication of their somewhat tentative nature.

In Table VI we present a summary of the ground and excited state vibrational assignments of this paper for h_{10}-anthracene.

TABLE VI. a_g and b_{1g} fundamentals of S_0 and S_1 h_{10}-anthracene.[b]

Vibrational mode		S_0 value (cm^{-1})	S_1 value (cm^{-1})
a_g:	12	390	385
	11	624	583
	10	753	755
	9	1012	1019
	8	1165	
	7	1263	1168
	6	1408	1380
	5	1486	1420
	4	1566	1501
b_{1g}:	$\overline{11}$	391[a]	232
	$\overline{10}$	524	473
	$\overline{9}$	912	889
	$\overline{8}$	1100	...
	$\overline{7}$	1183	1184
	$\overline{6}$	1274[a]	...
	$\overline{5}$	1382	1409
	$\overline{4}$	1576[a]	1514
	$\overline{3}$	1643	1635

[a] Reference 24.
[b] See the text for details of the assignments.

IV. SUMMARY

We have presented and analyzed fluorescence excitation and single vibronic level fluorescence (SVL) spectra of jet-cooled anthracene and some deuterated derivatives. Aided by the shape of the rotational contours and after having assessed influences of van der Waal's complexes, vibrationally hot molecules, and collisional interactions in observed spectra, we have analyzed vibrational structure primarily in terms of a_g and b_{1g} fundamentals. A comparison of h_{10}-anthracene vibrations in S_0 and S_1 appears in Table VI. The results presented here together with the vibrational assignments provide a basis for the work presented in other articles[8–10] which emphasize the dynamics of intramolecular vibrational coupling and energy redistribution in anthracene.

ACKNOWLEDGMENTS

It is a pleasure to acknowledge support of this work by the National Science Foundation. We also would like to thank Professor Ed Lee and Ms. Nancy Garland for their time and generous help with the rotational contour program.

[1] W. R. Lambert, P. M. Felker, and A. H. Zewail, J. Chem. Phys. **75**, 5958 (1981).
[2] (a) J. A. Syage, W. R. Lambert, P. M. Felker, A. H. Zewail, and R. M. Hochstrasser, Chem. Phys. Lett. **88**, 266 (1982); (b) P. M. Felker, Wm. R. Lambert, and A. H. Zewail, *ibid.* **89**, 309 (1982); (c) P. M. Felker, J. A. Syage, W. R. Lambert, and A. H. Zewail, *ibid.* **92**, 1 (1982); (d) P. M. Felker, W. R. Lambert, and A. H. Zewail, J. Chem. Phys. **77**, 1603 (1982); (e) P. M. Felker and A. H. Zewail, Chem. Phys. Lett. **94**, 448 (1983); **94**, 454 (1983); (f) P. M. Felker and A. H. Zewail, J. Chem. Phys. **78**, 5266 (1983); (g) P. M. Felker and A. H. Zewail, Chem. Phys. Lett. **102**, 113 (1983).
[3] G. J. Small, J. Chem. Phys. **52**, 656 (1970).
[4] A. Bree and S. Katagiri, J. Mol. Spectrosc. **17**, 24 (1965) and references therein.
[5] T. P. Carter and G. D. Gillispie, J. Phys. Chem. **86**, 2691 (1982).
[6] See, (for example) (a) R. St. Dygdala and K. Stefanski, Chem. Phys. **53**, 51 (1980); (b) S. O. Mirumyants, E. A. Vandyukov, and Yu. S. Demchuk, Opt. Spectrosc. **39**, 360 (1975).
[7] T. R. Hays, W. Henke, H. L. Selzle, and E. W. Schlag, Chem. Phys. Lett. **77**, 19 (1981).
[8] W. R. Lambert, P. M. Felker, and A. H. Zewail, J. Chem. Phys. **81**, 2209 (1984).
[9] W. R. Lambert, P. M. Felker, and A. H. Zewail, J. Chem. Phys. **81**, 2217 (1984).
[10] J. A. Syage, P. M. Felker, and A. H. Zewail, J. Chem. Phys. (to be published).
[11] (a) P. Langridge-Smith, D. Brumbaugh, C. Hyaman, and D. H. Levy, J. Phys. Chem. **85**, 3742 (1981), and references therein; (b) S. M. Beck, M. G. Liverman, D. L. Monts, and R. E. Smalley, J. Chem. Phys. **70**, 232 (1979).

Phys. Chem. **85**, 3742 (1981), and references therein; (b) S. M. Beck, M. G. Liverman, D. L. Monts, and R. E. Smalley, J. Chem. Phys. **70**, 232 (1979).
[12](a) S. M. Beck, D. E. Powers, J. B. Hopkins, and R. E. Smalley, J. Chem. Phys. **73**, 2019 (1980); (b) S. M. Beck, J. B. Hopkins D. E. Powers, and R. E. Smalley, *ibid.* **74**, 43 (1981) and references therein.
[13]A. Amirav, U. Even, and J. Jortner, J. Chem. Phys. **75**, 3770 (1981).
[14]A. Amirav, U. Even, and J. Jortner, Chem. Phys. Lett. **72**, 21 (1980).
[15]E. F. Zalewski, R. A. Keller, and R. Engleman, Jr., J. Chem. Phys. **70**, 1015 (1979), and references therein.
[16]J. L. Charlton and R. Agagnier, Can. J. Chem. **51**, 1852 (1973).
[17]R. Pariser, J. Chem. Phys. **24**, 250 (1956).
[18]R. S. Mulliken, J. Chem. Phys. **23**, 1997 (1955).
[19]H. Selzle, W. E. Howard, and E. W. Schlag, *Rotational Band Contour Program* from Technische Universitat Munchen.
[20]W. R. Lambert, Ph. D. thesis, California Institute of Technology (1982).
[21]B. N. Cyvin and S. J. Cyvin, J. Phys. Chem. **73**, 1430 (1969).
[22](a) D. P. Craig and P. C. Hobbins, J. Chem. Soc. 2309 (1955); (b) J. Sidman, J. Chem. Phys. **25**, 115 (1956).
[23]See, for example, S. F. Fischer and E. C. Lim, Chem. Phys. Lett. **26**, 312 (1974).
[24]J. Räsänen, F. Stenman, and Eeva Penttinen, Spectrochim. Acta. Part A **29**, 395 (1973).
[25]See, for example, (a) A. Amirav, U. Even, and J. Jortner, Chem. Phys. **51**, 31 (1980); (b) E. Kolodney and A. Amirav, *ibid.* (submitted for publication).
[26]K. Ohno, J. Mol. Spectrosc. **77**, 329 (1979).
[27]R. P. Rava and L. Goodman, J. Phys. Chem. **86**, 480 (1982), and references therein.
[28]G. Neerland, B. N. Cyvin, J. Brunvoll, S. J. Cyvin, and P. Klaeboe, Z. Naturforsch. Teil. A, **35**, 1390 (1980).